7-1-2006

Transport of galectin-3 between the nucleus and cytoplasm. II. Identification of the signal for nuclear export

Su Yin Li
Michigan State University

Peter J. Davidson
Michigan State University

Nancy Y. Lin
Michigan State University

Ronald J. Patterson
Michigan State University

Glycobiology vol. 16 no. 7 pp. 612–622, 2006
doi:10.1093/glycob/cwj089
Advance Access publication on February 9, 2006

Transport of galectin-3 between the nucleus and cytoplasm. II. Identification of the signal for nuclear export

Su-Yin Li[2], Peter J. Davidson[3], Nancy Y. Lin[2], Ronald J. Patterson[4], John L. Wang[2], and Eric J. Arnoys[1,5]

[2]Department of Biochemistry, [3]Cell and Molecular Biology Program, and [4]Department of Microbiology, Michigan State University, East Lansing, MI 48824; and [5]Department of Chemistry and Biochemistry, Calvin College, Grand Rapids, MI 49546

Received on December 7, 2005; revised on January 25, 2006; accepted on February 3, 2006

Galectin-3, a factor involved in the splicing of pre-mRNA, shuttles between the nucleus and the cytoplasm. Previous studies have shown that incubation of fibroblasts with leptomycin B resulted in the accumulation of galectin-3 in the nucleus, suggesting that the export of galectin-3 from the nucleus may be mediated by the CRM1 receptor. A candidate nuclear export signal fitting the consensus sequence recognized by CRM1 can be found between residues 240 and 255 of the murine galectin-3 sequence. This sequence was engineered into the pRev(1.4) reporter system, in which candidate sequences can be tested for nuclear export activity in terms of counteracting the nuclear localization signal present in the Rev(1.4) protein. Rev(1.4)–galectin-3(240–255) exhibited nuclear export activity that was sensitive to inhibition by leptomycin B. Site-directed mutagenesis of Leu247 and Ile249 in the galectin-3 nuclear export signal decreased nuclear export activity, consistent with the notion that these two positions correspond to the critical residues identified in the nuclear export signal of the cAMP-dependent protein kinase inhibitor. The nuclear export signal activity was also analyzed in the context of a full-length galectin-3 fusion protein; galectin-3(1–263; L247A) showed more nuclear localization than wild-type, implicating Leu247 as critical to the function of the nuclear export signal. These results indicate that residues 240–255 of the galectin-3 polypeptide contain a leucine-rich nuclear export signal that overlaps with the region (residues 252–258) identified as important for nuclear localization.

Key words: galectins/nuclear export/nuclear import/nucleocytoplasmic transport/splicing factor

Introduction

Galectin-3 (Gal3) shuttles between the nucleus and cytoplasm of cells (Davidson *et al*., 2002). As a splicing factor (Dagher *et al*., 1995; Vyakarnam *et al*., 1997), Gal3 must be imported into the nucleus, where its substrate, pre-mRNA, is localized. Conversely, its export from the nucleus to the cytoplasm has been shown to be important for a number of biological activities. For example, wild-type Gal3 can be phosphorylated at Ser 6 and, in response to apoptotic insults, the phosphorylated Gal3 is exported from the nucleus to the cytoplasm and protects the cells from drug-induced apoptosis (Takenaka *et al*., 2004). A serine-to-alanine mutant at residue 6 (S6A) could not be phosphorylated; the nonphosphorylated polypeptide was not exported from the nucleus and failed to protect the cells from apoptosis. It has also been reported that Gal3 interacts with the protein Sufu (Suppressor of fused), a negative regulator of the Hedgehog signal transduction pathway that interacts directly with the Gli family of transcription factors (Paces-Fessy *et al*., 2004). The Sufu polypeptide contains a functional leucine-rich nuclear export signal (NES), and the fusion protein derived from Sufu and green fluorescent protein (GFP) is found predominantly in the cytoplasm of transfected HeLa cells. As expected, mutants of Sufu in which the NES has been inactivated [Sufu(L383A; L385A)] localized mostly to the nucleus. When cotransfected with Gal3, however, the same Sufu(L383A; L385A) mutant was found in the cytoplasm, colocalized with Gal3. Thus, the possibility is raised that Gal3 plays a role in the nuclear versus cytoplasmic distribution of a transcriptional regulator.

Using digitonin-permeabilized mouse 3T3 fibroblasts, we had previously documented that Gal3 is selectively exported from the nucleus (Tsay *et al*., 1999). This export was temperature dependent and could be blocked by the addition of wheat germ agglutinin, which binds to the nuclear pore protein p62. In addition, we also showed that incubation of mouse and human fibroblasts with leptomycin B (LMB) resulted in the accumulation of Gal3 in the nuclei of the treated cells (Tsay *et al*., 1999; Openo *et al*., 2000). Similar effects of LMB were also observed in human carcinoma cell lines, HeLa and BT-549 (Paces-Fessy *et al*., 2004; Takenaka *et al*., 2004). LMB binds to and inhibits the activity of the nuclear export receptor, CRM1, which recognizes a leucine-rich NES on the cargo (Ossareh-Nazari *et al*., 1997; Kudo *et al*., 1998). These results suggest that Gal3 is exported through the nuclear pore complex by a receptor-mediated pathway involving CRM1.

The nuclear versus cytoplasmic distribution of the protein must represent some balance between nuclear import versus export as well as mechanism(s) of retention in either one of the compartments, through cytoplasmic anchorage or binding to a nuclear component. As a first step in understanding how these four parameters determine the nuclear versus cytoplasmic distribution of Gal3, a series of studies were carried out to identify the residues in the Gal3 polypeptide critical for nuclear import and export in the

[1]To whom correspondence should be addressed; e-mail: earnoys@calvin.edu

shuttling process. Studies identifying the amino acid sequence required for nuclear import are reported in Davidson *et al*. (2006). In this study, we present evidence for a leucine-rich NES at the COOH-terminal portion of the protein.

Results

The Rev(1.4)–GFP vector for the analysis of a functional NES

Previous studies had documented that treatment of mouse and human fibroblasts with LMB resulted in the accumulation of Gal3 in the nucleus, as revealed by accentuation of the nuclear staining (Tsay *et al*., 1999; Openo *et al*., 2000). Moreover, in Davidson *et al*. (2006), we have also shown that the GFP–MBP–Gal3(1–263) construct behaved in the same way as endogenous Gal3 in terms of its response to LMB by accumulating in the nucleus. These results all suggest that LMB inhibited the export of Gal3 from the nucleus and that this latter process was mediated by the CRM1 exportin, which recognizes leucine-rich NESs (Ossareh-Nazari *et al*., 1997). Indeed, a putative leucine-rich NES, with requisite spacing of leucine/isoleucine residues, can be identified between residues 240 and 255 of the murine Gal3 sequence (Figure 1C, line 5). Moreover, this NES motif appears to be conserved in the Gal3 homologs of various species.

To test whether this putative NES is indeed functional, we have taken advantage of the pRev(1.4)–GFP vector (Henderson and Eleftheriou, 2000). Although the HIV-1 Rev protein normally contains both a nuclear localization signal (NLS) and a NES, the Rev(1.4) variant is NES deficient. Instead, test sequences representing a putative NES can be cloned in frame between the Rev(1.4) segment and the GFP reporter (see schematic in Figure 1A). The fusion protein expressed by this vector contains the NLS of Rev, whose nuclear import activity could be decreased by treatment of cells with actinomycin D (ActD) (Kalland *et al*., 1994; Meyer and Malim, 1994). This allows the activity of very weak NESs to be detected. Thus, the relative activity of different NESs can be distinguished by their ability to shift the fusion protein to the cytoplasm, both in the presence and in the absence of active nuclear import (i.e., in the absence and presence of ActD, respectively). If the test NES is recognized by the CRM1 exportin, then nuclear export is expected to be sensitive to LMB inhibition (Ossareh-Nazari *et al*., 1997; Kudo *et al*., 1998).

On the basis of this, ActD and LMB played critical roles in our dissection of the NLS-based nuclear import and the CRM1-mediated nuclear export of fusion proteins derived from the Rev(1.4)–GFP vector (Figure 1B). In addition, to obviate any complications arising from newly synthesized proteins bearing the GFP reporter, the ActD and LMB experiments were always carried out in the presence of cycloheximide (CHX). Therefore, we first tested the effects of the three drugs on the nuclear versus cytoplasmic distribution of endogenous Gal3, as revealed by staining with anti-Gal3 antibodies. Neither CHX (10 μg/ml) nor ActD (5 μg/ml), alone or in combination, altered the nuclear and cytoplasmic localization of Gal3 in 3T3 cells. On the other hand, treatment of the same cells with LMB at a concentration as low as 5.4 ng/ml (10 nM) resulted in the accumulation of Gal3 in the nucleus, as was reported previously (Tsay *et al*., 1999). This effect of LMB was also observed in

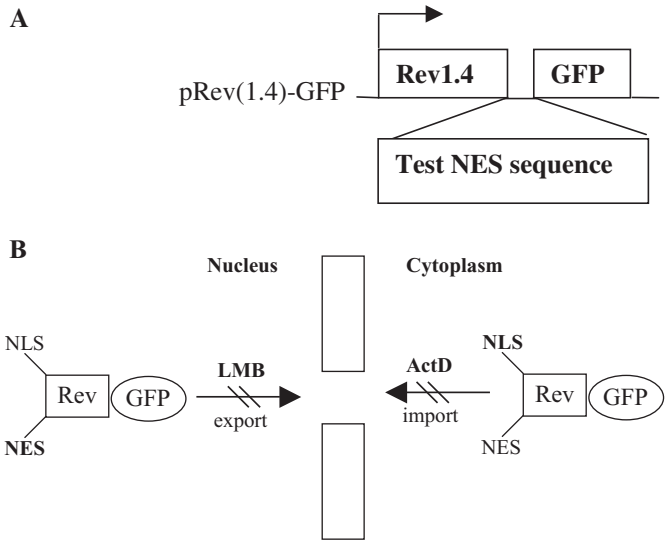

C

Construct	Test NES sequence	comment
GFP		GFP-N1(No NLS; No NES)
Rev1.4	NONE	NLS but No NES
PKI NES	33- N S N E L A L K L A G L D I N K T E	residues 33-50 of PKI
IκB-α NES	261-P S T R I Q Q Q L G Q L T L E N L Q	residues 261-278 of IκB-α
Gal3 NES	240- N L R E I S Q L G I S G D I T L	residues 240-255 of Gal3
Gal3 NES (I244A; L247A)	A A	residue 244: mutate I to A residue 247: mutate L to A
Gal3 NES (L247A; I249A)	A A	residue 247: mutate L to A residue 249: mutate I to A

Fig. 1. (**A**) Schematic diagram of the pRev(1.4)–GFP vector for testing potential nuclear export signals (NESs). A potential NES is cloned into this vector for the expression of a fusion protein containing Rev(1.4)-test-sequence-GFP. Normal Rev has both an NLS and a NES; the Rev(1.4) variant is NES deficient. The expressed fusion protein uses the NLS of Rev to import the reporter into the nucleus. The activity of the potential NES to export the reporter is measured in terms of the nuclear and/or cytoplasmic distribution of the GFP fluorescence. (**B**) Schematic diagram illustrating the basis of the assay to determine the nuclear export activity of a potential NES. The NLS of the fusion protein is responsible for nuclear import and is highlighted by boldface type in the cytoplasm; this NLS-mediated import is reduced by treatment of cells with ActD. The NES of the fusion protein is responsible for nuclear export and is highlighted by boldface type in the nucleus; nuclear export mediated by leucine-rich NES is specifically blocked by leptomycin B (LMB). (**C**) Summary of the contents of the fusion proteins expressed by various constructs. The construct designated as GFP is simply the mammalian expression vector for the production of GFP. The construct designated as Rev1.4 expresses a NES-deficient variant of Rev as a fusion protein with GFP. The construct designated as PKI NES expresses the Rev(1.4)–GFP fusion protein containing the specific NES sequence shown, derived from PKI. Similarly, the other constructs express the Rev(1.4)–GFP fusion protein containing the specific test NES sequence shown.

the presence of CHX (Davidson *et al.*, 2006) or a combination of CHX and ActD (data not shown).

Cultures of 3T3 cells were transfected with the construct expressing the Rev(1.4)–GFP fusion protein (~40 kDa). In the absence of ActD, a majority of the fluorescent cells exhibited the N-labeling pattern (Figures 2A and 3). It should be noted that the fluorescence image of this N-labeling pattern (Figure 2A) is particularly sharp and focused on the nucleolus, reflecting the properties of the NLS in Rev(1.4)–GFP (Kalland *et al.*, 1994; Meyer and Malim, 1994). Addition of CHX and ActD resulted in more of the fusion protein in the cytoplasm, as demonstrated by a shift in the histogram of fluorescence distributions to the right, at the expense of the N-labeling pattern (Figure 3). This is consistent with the notion that the Rev(1.4)–GFP polypeptide contains an NLS whose activity could be decreased by ActD (Figure 1B) (Kalland *et al.*, 1994; Meyer and Malim, 1994).

We also tested the effect of inserting test NES sequences whose strengths had been previously characterized (Henderson and Eleftheriou, 2000). In all of the cells transfected with the Rev(1.4)–GFP vector containing the NES of protein kinase inhibitor (PKI) as the test sequence, the fluorescence labeling pattern was exclusively C, cytoplasmic (Figure 2B). This was true irrespective of whether CHX and ActD were included in the cultures (Figure 3). Thus, the PKI NES was sufficiently strong to overcome an active NLS (Figure 1C, line 3). The NES of IκBα (Figure 1C, line 4) could neutralize an active NLS, resulting in a majority of the cells exhibiting the N ~ C labeling pattern in the absence of ActD

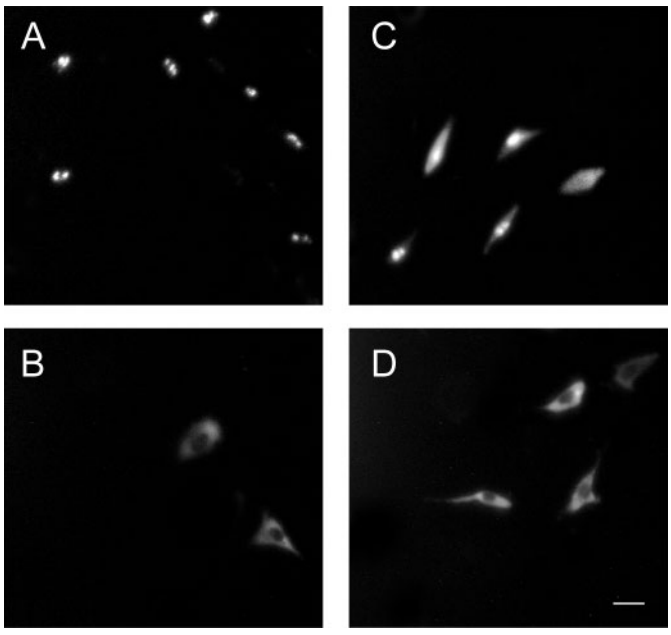

Fig. 2. Representative fluorescence micrographs illustrating the GFP localization patterns obtained with various test NES sequences in the pRev(1.4)–GFP vector. (**A**) Cells expressing Rev(1.4)–GFP protein, most of which yielded sharp nucleolar fluorescence pattern. (**B**) Cells expressing Rev(1.4)–GFP containing the NES of PKI, which yielded the C-fluorescence pattern. (**C**) Cells expressing Rev(1.4)–GFP containing the NES of IκBα, which yielded the N > C and N ~ C fluorescence patterns. (**D**) Cells, in the presence of CHX (10 μg/ml) and ActD (5 μg/ml), expressing Rev(1.4)–GFP containing the NES of IκBα, many of which yielded the C-fluorescence pattern. Bar = 50 μm.

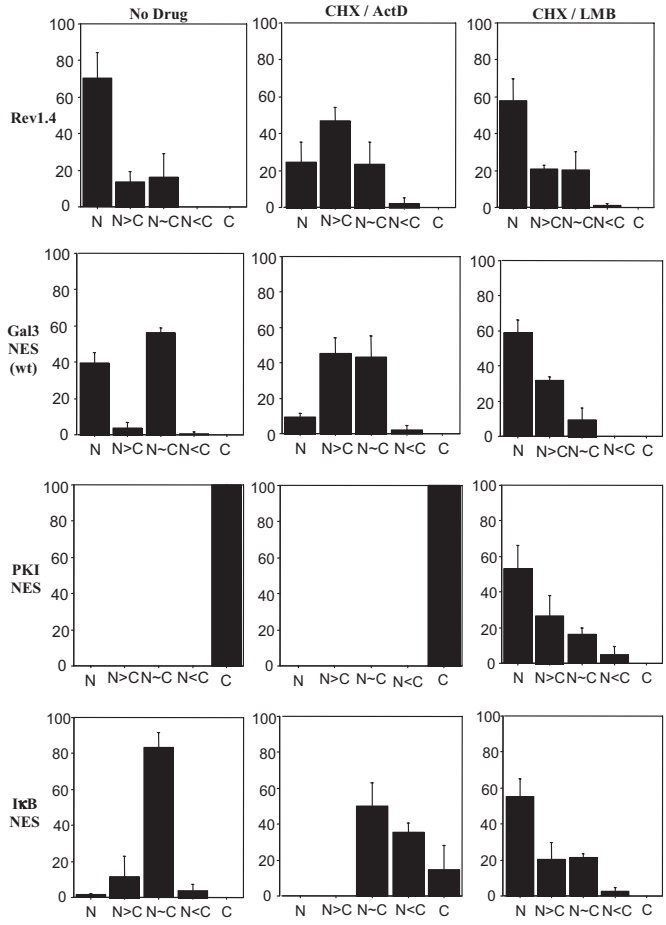

Fig. 3. Histograms showing the distribution of cells with fluorescence patterns N, N > C, N ~ C, N < C, and C. The constructs used for the transfections are indicated on the left-hand side of each row. The conditions (no drug addition, CHX [10 μg/ml], ActD [5 μg/ml], and LMB [5.4 ng/ml]) are indicated at the top of each column. The data represent the averages of triplicate determinations with standard error of the mean.

(Figures 2C and 3). In the presence of ActD, the histogram shifts to the right, with about half of the cells showing either an N < C or an exclusively C fluorescence pattern (Figures 2D and 3), because the NLS activity has been decreased.

Analysis of the Gal3 NES in the Rev(1.4)–GFP vector

When the putative NES of Gal3 was inserted into the Rev(1.4)–GFP vector as the test sequence (Figure 1C, line 5), we found fluorescence in both the nucleus and the cytoplasm (Figure 4A). The pattern was quite distinct from the sharp fluorescence focused in the nucleolus observed for the Rev(1.4)–GFP vector devoid of any NES (Figure 2A). Although a thorough analysis required quantitation via histograms, the qualitative difference in fluorescence patterns (Figure 2A vs. Figure 4A) strongly illustrated nuclear export due to the putative NES of Gal3. Even when a particular cell was scored in the N (exclusively nuclear) category, the fluorescence due to the fusion protein expressed from Rev(1.4)–GFP was sharply nucleolar (Figure 2A), whereas the fluorescence from Rev(1.4)-Gal3 NES-GFP was diffusely spread in the nucleoplasm (Figure 4A).

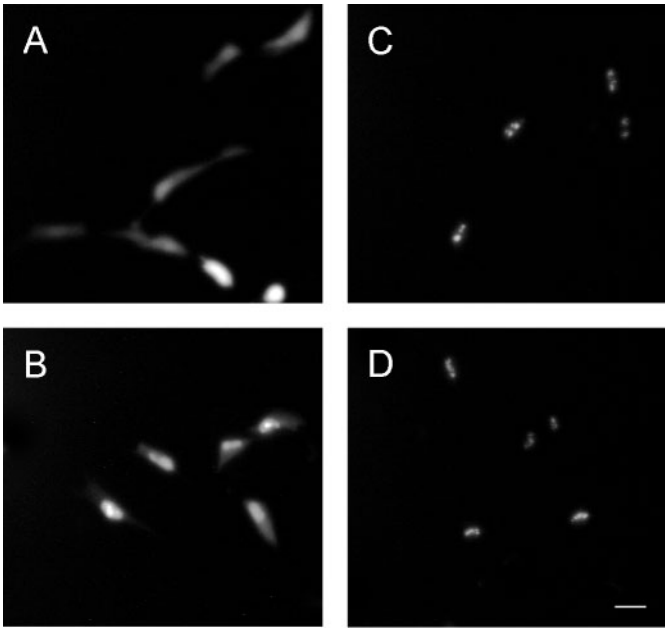

Fig. 4. Representative fluorescence micrographs showing the nuclear versus cytoplasmic distribution of Rev(1.4)–GFP protein containing the NES sequence of Gal3 or site-directed mutants. (**A**) Cells expressing Gal3 NES (wt) in the absence of drugs. (**B**) Cells expressing Gal3 NES (wt) incubated in the presence of CHX (10 μg/ml) and ActD (5 μg/ml). (**C**) Cells expressing Gal3 NES (wt) incubated in the presence of CHX (10 μg/ml) and LMB (5.4 ng/ml). (**D**) Cells expressing Gal3 NES (L247A; I249A) in the absence of drugs. Bar = 50 μm.

Considering the histograms of Gal3 NES transfected cells, a little more than half showed the N ~ C fluorescence pattern (Figure 3). This distribution should be compared with the corresponding distribution obtained in the transfection with the Rev(1.4)–GFP vector, which showed predominantly N labeling. When these two histogram distributions were subjected to a chi-square test, the differences were found to be significant ($p < 0.0001$). Although these results indicate that a functional NES resides in the Gal3 sequence, the activity of this NES appeared weaker than that of the IκBα NES, neutralizing the effect of the active nuclear import in only half of the cells.

When nuclear import was inhibited by the addition of CHX and ActD, cytoplasmic localization was even more pronounced in cells transfected with Gal3 NES (Figures 3 and 4B). Thus, the NES activity of the Gal3 sequence becomes more apparent when nuclear import is inactivated. A chi-square analysis of Gal3 NES (wt) (no drug) versus Gal3 NES (wt) (CHX/ActD) revealed a significant difference ($p < 0.0001$) between the two conditions.

The effect of LMB on the fluorescence distribution

The Gal3 NES activity, as reported by the pRev(1.4)–GFP vector, should be sensitive to LMB inhibition, as had been documented for endogenous Gal3 of mouse and human fibroblasts (Tsay *et al.*, 1999; Openo *et al.*, 2000). Indeed, incubation with CHX and LMB shifted the distribution in favor of the nucleus, yielding sharp nucleolar fluorescence (Figure 4C), similar to that observed with Rev(1.4)–GFP containing no NES (Figure 2A). A vast majority of the cells showed an exclusively N or the N > C fluorescence pattern (Figure 3). Chi-square analysis of the data revealed significant differences between (a) Gal3 NES (wt) (no drug) versus Gal3 NES (wt) (CHX/LMB) ($p < 0.0001$) and (b) Gal3 NES (wt) (CHX/ActD) versus Gal3 NES (wt) (CHX/LMB) ($p < 0.0001$).

Although 60 cells on average yielded the N-labeling pattern, there were always a few that showed N ~ C (Figure 3). When 3T3 cells were incubated with LMB, they accumulated endogenous Gal3 in the nucleus, as reflected by an accentuation of the nuclear staining (Tsay *et al.*, 1999); however, there was always some cytoplasmic fluorescence in these LMB-treated cells. This was also the case when the effect of LMB was studied using the GFP–MBP–Gal3(1–263) reporter (Davidson *et al.*, 2006).

Addition of CHX and LMB also affected the fluorescence of other test NES sequences, shifting the distribution in favor of the exclusively nuclear (N) pattern. In the presence of LMB, about half of the PKI NES showed the N-labeling pattern; this should be compared with the exclusively cytoplasmic (C) pattern obtained in the absence of the export inhibitor (Figure 3). Similarly, LMB shifted the fluorescence distribution for the IκBα test NES sequence, from a predominantly N ~ C labeling pattern to about half with exclusively N pattern (Figure 3). In both cases, the effects of CHX and LMB were partial; not all of the cells showed an exclusively N-labeling pattern.

Finally, the Rev(1.4)–GFP construct contains no NES; therefore, it should not be sensitive to LMB. Consistent with this notion, CHX and LMB did not shift the fluorescence distribution of the Rev(1.4)–GFP fusion protein in favor of a more N-labeling pattern than the no-drug control (Figure 3).

Site-directed mutagenesis of the Gal3 NES

Site-directed mutagenesis was carried out to test the effect of mutagenizing leucine 247 to alanine (L247A) and isoleucine 249 to alanine (I249A). These two residues were chosen because they occupy corresponding positions that had been shown to be critical for the functioning of the leucine-rich NES in PKI (Wen *et al.*, 1995). The fluorescence pattern of this mutant (Figure 4D), designated Gal3 NES (L247A; I249A), is similar to that of Rev(1.4)–GFP which carried no NES (Figure 2A). The histograms of Gal3 NES (L247; I249A) also more closely resembled those of the Rev(1.4)–GFP (Figure 5). In the absence of any drugs, a higher number of cells exhibited the N-labeling pattern in both the Rev(1.4)–GFP and Gal3 NES (L247A; I249A) fusion proteins, compared with the 40-cell to 60-cell split between N and N ~ C labeling pattern observed in Gal3 NES (wt) ($p<0.0001$). The effect of CHX/ActD on Gal3 NES (L247A; I249A) was also comparable to the effect of the drugs on Rev(1.4)–GFP (Figure 5). The following chi-square analyses in the column labeled CHX/ActD in Figure 5 were particularly instructive: (a) Rev(1.4) (CHX/ActD) versus Gal3 NES (wt) (CHX/ActD), $p < 0.0001$; (b) Rev(1.4) (CHX/ActD) versus Gal3 NES (L247A; I249A) (CHX/ActD), $p = 0.0157$; (c) Gal3 NES (wt) (CHX/ActD) versus Gal3 NES (L247A; I249A) (CHX/ActD), $p < 0.0001$.

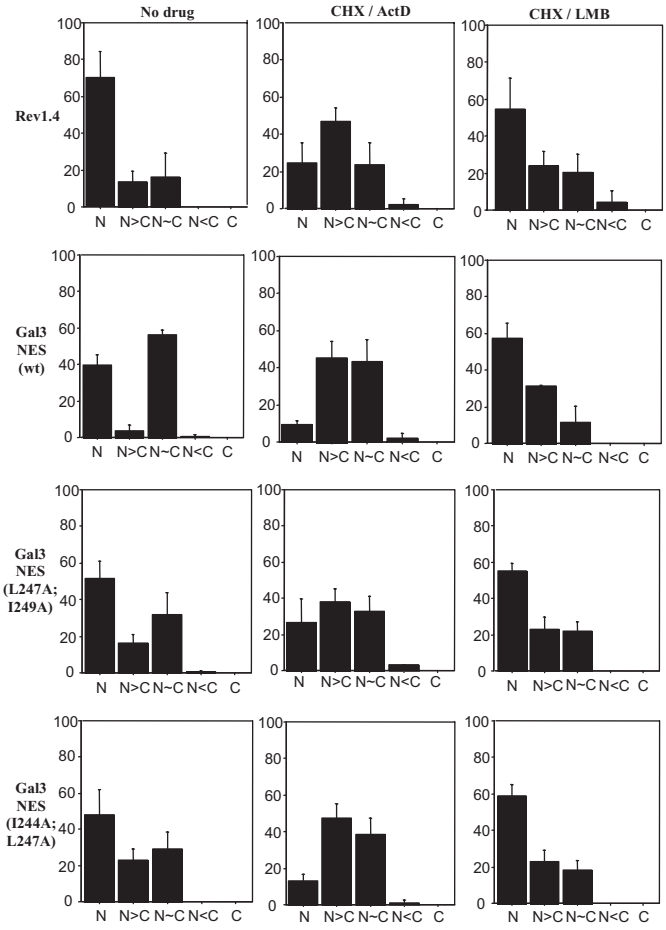

Fig. 5. A comparison of the histogram distributions of cells with various fluorescence patterns for Gal3 NES (wt), Gal3 NES (I244A; L247A), and Gal3 NES (L247A; I249A). The constructs used for each transfection are indicated at the left-hand side of each row. Transfected cells were incubated in the absence of drugs (No drug), the presence of CHX (10 μg/ml) and ActD (5 μg/ml) (CHX/ActD), or the presence of CHX (10 μg/ml) and LMB (5.4 ng/ml) (CHX/LMB). The data represent the averages of triplicate determinations with standard error of the mean.

Finally, the histograms of Gal3 NES (L247A; I249A) showed little change upon addition of CHX/LMB (Figure 5). If the leucine-rich NES were disrupted by the L247A and I249A mutations, one would not expect a dramatic shift toward more nuclear staining upon LMB inhibition of CRM1. Chi-square analysis showed that the histogram distributions were not significantly different for (a) Gal3 NES (L247A; I249A) (no drug) versus Gal3 NES (L247A; I249A) (CHX/LMB) ($p = 0.005$) and (b) Rev(1.4) (CHX/LMB) versus Gal3 NES (L247A; I249A) (CHX/LMB) ($p = 0.0034$).

In the course of these studies, the Gal3 NES (I244A; L247A) mutant was also generated. In the absence of any drugs, the histograms of fluorescence distribution were different for Gal3 NES (wt) and Gal3 NES (I244A; L247A) ($p < 0.0001$). On the other hand, the histograms for Gal3 NES (L247A; I249A) and Gal3 NES (I244A; L247A) were not significantly different ($p = 0.0093$). This would be consistent with the results obtained with the NES of PKI, in which mutation of a single critical residue yielded the similar effects on export activity as the double mutant (Wen *et al.*, 1995). In the present analysis, the Gal3 NES (I244A; L247A) mutant would hit the critical L247 in the same way as the Gal3 NES (L247A; I249A) double mutant. In accord with this notion, the histograms of fluorescence distribution for Gal3 NES (L247A; I249A) (CHX/ActD) and Gal3 NES (I244A; L247A) (CHX/ActD) were not significantly different ($p = 0.0013$) when the NLS activity was inhibited (Figure 5).

Analysis of the NES in the context of the Gal3 polypeptide

Although the above data suggest that residues 240–255 of the Gal3 sequence exhibit NES activity when tested in isolation, we wanted to make use of the availability of the GFP–MBP–Gal3(1–263) construct (Davidson *et al.*, 2006) to test whether it was functional in the context of the Gal3 polypeptide. We first engineered the double mutant GFP–MBP–Gal3(1–263; L247A; I249A). If the putative NES was indeed functional in CRM1-mediated nuclear export, we would expect the fusion protein expressed by the mutant construct to exhibit a nuclear localization. Transfection of 3T3 cells with the mutant construct resulted, however, in a mostly cytoplasmic fluorescence pattern (Figure 6B). Whereas a majority of the cells transfected with the wild-type construct [GFP–MBP–Gal3(1–263) showed a predominantly nuclear localization, most of the cells transfected with the double mutant showed cytoplasmic fluorescence (Figure 6C).

DNA sequence analysis confirmed that the mutations had been correctly carried out. Lysates derived from the transfected cultures were subjected to SDS–PAGE and immunoblotting. Antibodies directed against all three parts of the fusion protein (GFP, MBP, and Gal3) yielded the same results. The most prominent band was observed at ~100 kDa, corresponding to the expected molecular weights of the wild-type and mutant polypeptides (Figure 6A). We interpret the results to indicate that this stretch of the Gal3 sequence, containing the putative NES, borders the region important for nuclear import and that our mutagenesis on residues 247 and 249 diminished nuclear import. This notion is consistent with the results of our analysis of a nuclear localization sequence of Gal3, which implicated seven amino acids near the carboxyl-terminus as necessary for nuclear import (Davidson *et al.*, 2006).

In light of the results obtained with Gal3 NES (I244A; L247A) in the Rev(1.4)–GFP vector, in which it appeared that mutation of a single critical residue (L247A) affected NES activity (Figure 5), we also tested the effect of this mutation in the GFP–MBP–Gal3 fusion protein. The histogram of fluorescence distribution of GFP–MBP–Gal3(1–263; L247A)-transfected cultures was different from that of the wild-type ($p < 0.0001$); there was a higher percentage of cells with a more nuclear localization (Figure 6C). This would be consistent with the notion that leucine 247 was critical to the function of the NES, as was found in the Rev(1.4)–GFP assay.

In contrast, the single mutation at residue 249 (isoleucine to alanine) appeared to have affected nuclear import, shifting the histogram of fluorescence distribution to the right (Figure 6) and making it more difficult to discern its direct effect on the NES. This may account, at least in part, for

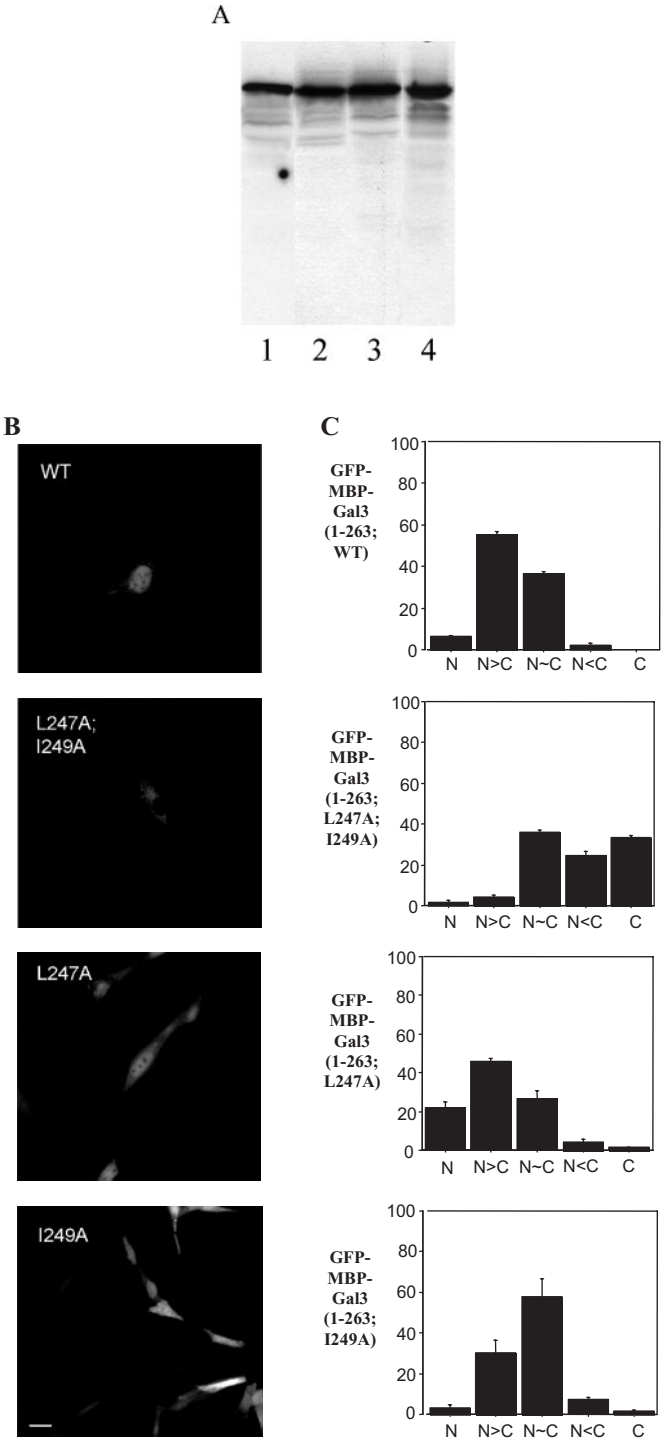

Fig. 6. Comparison of the properties of GFP–MBP–Gal3 fusion proteins bearing the wild-type sequence, double mutations at Leu247 and Ile249, a single mutation at Leu247, and a single mutation at Ile249. (**A**) Western blots of lysates of transfected cells, using antibodies directed against GFP. Lane 1, GFP–MBP–Gal3 (1–263); lane 2, GFP–MBP–Gal3(1–263; L247A; I249A); lane 3, GFP–MBP–Gal3 (1–263; L247A); and lane 4, GFP–MBP–Gal3 (1–263; I249A). (**B**) Representative fluorescence micrographs illustrating the GFP localization patterns. Bar = 10 μm. (**C**) Histograms showing the distribution of cells with the indicated fluorescence patterns.

the cytoplasmic localization of the double mutant, GFP–MBP–Gal3(1–263; L247A; I249A). Nevertheless, chi-square analysis of the histograms revealed significant differences ($p < 0.0001$) between GFP–MBP–Gal3(1–263; I249A) and (a) GFP–MBP–Gal3(1–263), (b) GFP–MBP–Gal3(1–263; L247A; I249A), and (c) GFP–MBP–Gal3(1–263; L247A).

NetNES predictor analysis of the Gal3 sequence

The amino acid sequence of murine Gal3 was submitted to the NetNES server (la Cour *et al*., 2004) to evaluate how its experimentally determined NES compared with the large database of other available NESs. NetNES predicted a NES that included L247, G248, and I249 of the Gal3 construct used in our studies (data not shown), perfectly matching the anchor residues of the experimentally determined NES. This region of the Gal3 polypeptide is within the carbohydrate-recognition domain (CRD), whose three-dimensional structure has been elucidated to 1.4 Å for the human homolog (Sorme *et al*., 2005). This structure offers another point of comparison to the collection examined by la Cour *et al*. (2004).

In human Gal3, residues corresponding to our L241 and I244, the first two hydrophobic amino acids in the NES, are found on either end of the sole α-helix of the CRD (Figure 7A). Residues corresponding to L247 and I249, the anchor residues in the NES, are found in an adjacent β-sheet. However, as was found with the majority of structures examined

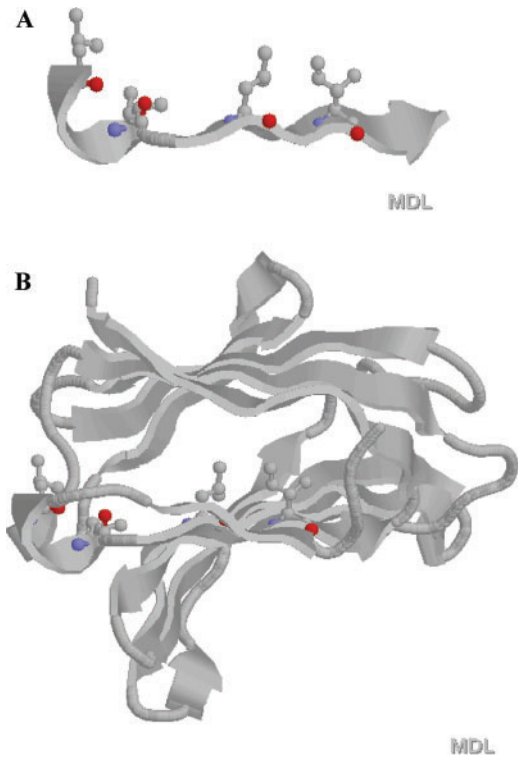

Fig. 7. Structural analysis of the NES of Gal3. (**A**) Hydrophobic residues of the NES (corresponding to murines L241, I244, L247, and I249), shown in ball-and-stick representation, align on the same face of the structure in a ribbon diagram of a portion of human Gal3. (**B**) A top view of the entire CRD of human Gal3 shows the NES buried in the interior of a β-sandwich motif.

by la Cour *et al.* (2004), all of the R groups are nearly parallel and are found on the same face of the structure. Not surprisingly, the NES is immersed within the hydrophobic β-sandwich motif of the CRD, though it is close to one of its edges (Figure 7B).

Discussion

The key findings of the present study include the following: (a) the Gal3 polypeptide carries a functional NES; (b) this NES fits the consensus sequence, with requisite spacing of Leu and Ile residues, recognized by the CRM1 exportin, and is sensitive to inhibition by LMB; and (c) the position of this NES, between residues 240–255, overlaps with the region of the Gal3 polypeptide critical for nuclear import of the protein.

In a recent computational study, la Cour *et al.* (2004) compared the primary, secondary, and tertiary structures of a number of leucine-rich NESs. Three key features were noted. First, in addition to hydrophobic amino acids, NESs tend to be enriched in glutamate, aspartate, serine, and glutamine, residues that are highly flexible and that could provide a mechanism for surface exposure of the NES. Second, the spacing of the hydrophobic residues in the canonical sequence [$Lx_{2-3}Lx_{(2-3)}LxL$] suggested amphipathic structures, allowing the hydrophobic residues to be aligned along one face of the folded protein. This was further confirmed by examination of the solved structures for nine regions containing NESs (la Cour *et al.*, 2004). Third, the NESs were located at or near a transition between two structural elements, with the signal starting in an α-helix and either remaining in an α-helix or continuing on to a β-structure. Manual inspection of the three-dimensional structures of the NESs of additional proteins not studied by la Cour *et al.* reveals that PKIα (Hauer *et al.*, 1999), p53 (Stommel *et al.*, 1999), 14-3-3 (Brunet *et al.*, 2002), and STAT1 (McBride *et al.*, 2000) also fit with their general conclusions.

The crystal structure of the CRD of the human homolog of Gal3 has been solved to 1.4 Å (Sorme *et al.*, 2005). The NES defined in this study (residues 240–255) strictly conforms to the parameters outlined by la Cour *et al.* (2004): the hydrophobic residues are positioned nearly parallel to each other, with the two N-terminal residues located within an α-helix and the last two in a β-sheet; the NES is found at a transition between two secondary structural elements; and the NES and flanking regions contain acidic residues and are enriched in serine (Figure 7A,B). Of the solved structures of confirmed NESs, Gal3 most closely resembles a NES in Smad1, an intracellular mediator of the transforming growth factor-β family cytokines that also shuttles between the nucleus and the cytoplasm (Xiao *et al.*, 2001; la Cour *et al.*, 2004). Both straddle an α-helix and a strand of a β-sheet. Furthermore, both NESs are buried within β-sandwich motifs.

The position of the NES, at the carboxyl-terminal portion of the Gal3 polypeptide, needs to be discussed in the context of other studies that suggest phosphorylation of serine 6 near the amino terminus was important for nuclear export. Although both phosphorylated and nonphosphorylated isoforms of Gal3 are found in the nuclear fraction, only phosphorylated Gal3 is identified in the exported fraction of a digitonin-permeabilized cell system (Tsay *et al.*, 1999). In addition, Takenaka *et al.* (2004) reported that a serine-to-alanine mutant at residue 6 could not be phosphorylated and that the nonphosphorylated polypeptide was not exported from the nucleus and failed to protect the cells from apoptotic insults due to chemotherapeutic drugs. The intriguing question is raised whether the NES near the carboxyl end can sense a conformational change induced by phosphorylation of residue 6 near the amino-terminal end, particularly in view of physicochemical data that suggest that the Gal3 polypeptide is delineated into two independently folded domains with distinct thermal melting temperatures (Agrwal *et al.*, 1993). Alternatively, phosphorylation could release Gal3 from an anchor that retains the protein in the nucleus. To the best of our knowledge, there are no data to suggest that the lectin activity of Gal3 affects or is affected by its intracellular localization.

The nuclear versus cytoplasmic distribution of Gal3 depends on the cell type. In baby hamster kidney (BHK) and Madin–Darby canine kidney (MDCK) cells, the protein is cytoplasmic (Sato *et al.*, 1993; Gaudin *et al.*, 2000). This cytoplasmic localization was observed both for the endogenous protein and for the protein overexpressed in the same cells transfected with a cDNA construct encoding the hamster polypeptide. Overexpression of the same cDNA in mouse 3T3 fibroblasts, however, resulted in a predominantly nuclear localization (Gaudin *et al.*, 2000). This cell-type difference in nuclear versus cytoplasmic distribution of Gal3 may reflect the presence or absence of an interacting partner that either has a potent NES or tethers it to a compartment-specific anchor. Indeed, it has been reported that the transcriptional regulator Sufu interacts with Gal3 and sequesters the latter in the cytoplasm when both proteins are cotransfected into HeLa cells (Paces-Fessy *et al.*, 2004).

The distribution of Gal3 between the nuclear and cytoplasmic compartments in a single cell type is also dependent on the proliferative state of the culture under analysis. For example, quiescent cultures of fibroblasts (serum starved or density inhibited) exhibit a predominantly cytoplasmic localization, whereas proliferative cultures of the same cells (serum stimulated or low-density cultures) show nuclear accumulation (Moutsatsos *et al.*, 1987). It has also been reported that nuclear exclusion and cytoplasmic localization of Gal3 are correlated with replicative senescence during in vitro culture of human fibroblasts (Openo *et al.*, 2000) and with disease progression in colon (Lotz *et al.*, 1993) and prostate (van den Brule *et al.*, 2000) carcinoma.

It should be noted that observations of an exclusively cytoplasmic localization of a protein in cells do not necessarily mean that it does not enter the nucleus. It may simply reflect a dynamic situation in which the rate of nuclear export far exceeds nuclear import such that in any steady-state observation the protein is apparently found only in the cytoplasm. There are now many examples in which an exclusively cytoplasmic localization of a protein is converted to nuclear pattern simply by inhibition of CRM1-mediated nuclear export using LMB: (a) the ubiquitin-protein ligase (E3), hRPF1/Nedd4 (Hamilton *et al.*, 2001); (b) the

mitogen-activated protein kinase interacting kinase Mnk1 (Parra-Palau *et al*., 2003); (c) several protein translation factors that shuttle between the nucleus and the cytoplasm (Bohnsack *et al*., 2002); (d) Dsh (dishevelled) (Itoh *et al*., 2005), which functions in the Wnt signal transduction pathway. We ourselves have observed that certain N-terminal deletion mutants of Gal3 (e.g., GFP constructs containing residues 136–263) were exclusively cytoplasmic in the absence of LMB but evenly distributed throughout the cell in the presence of LMB (Davidson *et al*., 2006). The identification of a region necessary for nuclear import (Davidson *et al*., 2006), the present study on the NES, and the nuclear accumulation of Gal3 in the presence of LMB (Tsay *et al*., 1999; Openo *et al*., 2000; Paces-Fessy *et al*., 2004; Takenaka *et al*., 2004) are all consistent with the documented nucleocytoplasmic shuttling of the protein (Davidson *et al*., 2002), as had been observed in other systems described above.

Henderson and Eleftheriou (2000) developed the Rev(1.4)–GFP reporter system for testing potential NES sequences. Each putative NES sequence is challenged to overcome the active NLS of the HIV-1 Rev protein such that the fusion protein localizes to the cytoplasm. Such a NES, classified as "strong," was found in proteins such as PKI, the mitogen-activated protein kinase kinase (MAPKK), and the c-Abl oncogene (Henderson and Eleftheriou, 2000). Some test NES sequences display "weak" nuclear export activity. These can partially neutralize the NLS of the Rev(1.4)–GFP reporter, resulting in nuclear and cytoplasmic localization of the fusion protein. In the presence of ActD, which decreases the NLS activity in the Rev(1.4)–GFP reporter, the fusion containing a weak NES shifts further to the cytoplasm in the majority of the cells. Very weak NESs cannot normally overcome the rate of Rev NLS-mediated nuclear import in the absence of ActD but are able to shift the GFP fluorescence partially to the cytoplasm in 20–50% of the cells when import is decreased by ActD. The tumor suppressor p53 and its hdm2 regulator each have a NES that fits this latter category.

This notion of ranking of NES strengths has received strong support from an entirely independent line of investigation. Using microinjection of defined recombinant export substrates, Heger *et al*. (2001) showed that different leucine-rich NESs varied dramatically in determining the kinetics of export in intact cells. Thus, the NES of PKI, classified as a strong NES by the pRev(1.4)–GFP assay (Henderson and Eleftheriou, 2000), was found to export its protein very "fast" (5–10 min) (Heger *et al*., 2001). On the other hand, p53 was found to contain a very weak NES by the Rev(1.4)–GFP reporter assay (Henderson and Eleftheriou, 2000), and indeed, it turned out to be very slow (>10 h) in the kinetic assay of Heger *et al*. (2001). More interestingly, the latter study also reported that cotransfection experiments revealed that proteins containing a fast NES inhibited the export and biological activity in vivo of proteins harboring a slower NES (Heger *et al*., 2001). Thus, the export of a protein harboring a leucine-rich NES could also depend on what other export substrates are present in competition for transport receptor/cofactor.

By the criteria established in the development of the Rev(1.4)–GFP test vector (Henderson and Eleftheriou, 2000), the NES of Gal3 (residues 240–255 tested) would fall in the weak category. This weak NES activity may be important for the nuclear function of the protein. A strong NES might result in futile shuttling of Gal3 between the nucleus and cytoplasm, whereas a weak NES would allow longer residence in the nucleus so that the protein can accumulate to sufficient concentrations to assemble into ribonucleoprotein (RNP) complexes for pre-mRNA splicing. This notion was first advanced to explain the very low affinity observed between IκBα and the CRM1 exportin (Lee and Hannink, 2001), which appears to be consistent with our own observation that its NES exhibits weak nuclear export activity in the Rev(1.4)–GFP assay system.

Under regulated conditions, the rate of nuclear export for Gal3 could be upgraded through binding to other proteins that carry their own NES. Two such interacting ligands of Gal3 in the nucleus are Sufu (Paces-Fessy *et al*., 2004) and β-catenin 1 (Shimura *et al*., 2004). Xpress-tagged Gal3 was predominantly nuclear when transfected into HeLa cells. When co-expressed with Sufu, however, nuclear Gal3 levels decreased and the protein accumulated in the cytoplasm where it is colocalized with Sufu (Paces-Fessy *et al*., 2004). Thus, it appears that nuclear export of Gal3 is increased through binding to Sufu which carries its own leucine-rich NES. Conversely, binding of a regulatory protein might induce a conformational change in Gal3, opening up the structure and increasing the solvent exposure of the NES which is immersed within a β-sandwich motif. An N-terminal deletion of Gal3 that disrupted β-sheets near the NES without harming the region necessary for nuclear import shifted the localization of fusion proteins to the cytoplasm (Davidson *et al*., 2006). In this way, a cell might modulate the intracellular localization of Gal3 by means of a transiently masked NES that may either be exposed to facilitate protein export or be hidden to trap it in the nucleus.

The other nuclear ligand of Gal3 that possesses its own NES is β-catenin, which plays a role in the Wnt signaling pathway (Shimura *et al*., 2004). Dissection of the polypeptide showed that the region of β-catenin required for nuclear export overlapped the region required for import (Koike *et al*., 2004). The exclusively cytoplasmic localization of GFP–MBP–Gal3(1–263; L274A, I249A) suggests that the two mutations may have disrupted the region critical for nuclear import. This, in turn, implies that, like β-catenin, the NLS and NES overlap in the Gal3 polypeptide. The M9, KNS, and HNS sequences represent other examples of overlapping signals, in which the same stretch of amino acid sequence is capable of mediating both nuclear import and nuclear export (Michael *et al*., 1995; Michael *et al*., 1997; Fan and Steitz, 1998). The M9 signal, a stretch of ~38 amino acids with critical glycine and proline residues, was identified in the hnRNP A1 protein and is responsible for its shuttling property between the nucleus and the cytoplasm. The 39-residue KNS shuttling signal was identified in the hnRNP K protein. For nuclear export, the critical residues include negatively charge acidic amino acids. Fan and Steitz (1998) identified a 33-residue sequence, designated HNS, responsible for the shuttling activity of HuR, an RNA-binding protein that can stabilize labile mRNAs containing AU-rich elements in their 3′-untranslated regions.

Finally, the purpose of shuttling the protein between the nucleus and the cytoplasm remains to be elucidated. In studying nuclear export of Gal3 using a permeabilized cell system, it was found that in the transported fraction, Gal3 is associated with high-molecular-weight complexes of ~650 kDa (Tsay *et al*., 1999). On the basis of our previous documentation that Gal3 is involved in pre-mRNA splicing (Dagher *et al*., 1995; Vyakarnam *et al*., 1997) and that its detection in the nucleus is sensitive to ribonuclease (Laing and Wang, 1988; Hubert *et al*., 1995), the possibility is raised that Gal3 is exported from the nucleus in the form of an RNP complex along with the processed mRNA. The intriguing question then is whether Gal3 plays a role in determining the stability of the mRNA or in targeting it to ribosomes for translation.

Materials and Methods

Site-directed mutagenesis of the putative NES sequence in the GFP–MBP–Gal3 fusion protein

The construction of the vector for expression of the fusion protein GFP–MBP–Gal3 has been described in Davidson *et al*. (2006). Site-directed mutagenesis was carried out with the QuikChange Site-Directed Mutagenesis Kit (Stratagene, La Jolla, CA) using the vector for GFP–MBP–Gal3 as template. The primers used for the specific mutations were, for L247A, 5′-GGT TAT GTC ACC ACT GAT CCC CGC TTG GCT GAT TTC CCG GAG-3′ and 5′-CTC CGG GAA ATC AGC CAA GCG GGG ATC AGT GGT GAC ATA ACC-3′, for I249A, 5′-CGG GAA ATC AGC CAA CTG GGG GCC AGT GGT GAC ATA ACC CTC-3′ and 5′-GAG GGT TAT GTC ACC ACT GGC CCC CAG TTG GCT GAT TTC CCG-3′, and, for L247A; I249A, 5′-CGG GAA ATC AGC CAA GCG GGG GCC AGT GGT GAC ATA ACC-3′ and 5′-GGT TAT GTC ACC ACT GGC CCC CGC TTG GCT GAT TTC CCG-3′.

The pRev(1.4)–GFP vector and variants

The pRev(1.4)–GFP vector (Figure 1A) and its application for testing potential NES sequences were developed by Henderson and Eleftheriou (2000). Two previously identified NESs were also used in our study as controls: (a) the NES of the inhibitor of cAMP-dependent protein kinase (PKI) was characterized as a strong NES (Figure 1C, line 3); and (b) the NES of IκBα represented weak NES activity (Figure 1C, line 4). Each of these sequences was cloned as short fragments between the BamHI and the AgeI sites of pRev(1.4)–GFP, sandwiched between the Rev and the GFP coding sequences.

The vector pRev(1.4)–GFP containing the putative NES sequence of Gal3 (residues 240–255) (Figure 1C, line 5) was derived from the pRev(1.4)–GFP vector containing the NES of PKI by site-directed mutagenesis in five steps, each of which changed multiple amino acids. Finally, two mutants of the Gal3 NES, designated Gal3 NES (I244A; L247A) and Gal3 NES (L247A; I249A), were derived from the wild-type Gal3 NES in the pRev(1.4)–GFP vector by site-directed mutagenesis (Figure 1C, lines 6 and 7). For Gal3 NES (I244A, L247A), the forward and reverse primers were, respectively, 5′-CCA AAC CTT CGA GAG GCA TCT CAG GCA GGT ATC AGT GGG-3′ and 5′-CCC ACT GAT ACC TGC CTG AGA TGC CTC TCG AAG GTT TGG-3′. For Gal3 NES (L247A; I249A), the primers were 5′-CGA GAG ATA TCT CAG GCA GGT GCC AGT GGG GAC ATC ACA C-3′ and 5′-G TGT GAT GTC CCC ACT GGC ACC TGC CTG AGA TAT CTC TCG-3′. All of these experiments used the QuikChange Site-Directed Mutagenesis Kit of Stratagene.

Cell culture and transfection

The conditions for the culture and transfection of NIH mouse 3T3 fibroblasts are detailed in Davidson *et al*. (2006). In the present experiment, the effects of various drugs on the nuclear versus cytoplasmic distribution of the reporter proteins were tested. At 9 h after transfection, either ActD and CHX or LMB and CHX were added to the samples. Samples receiving no drugs served as controls. After 5 h of treatment (14 h after transfection), the cells were observed under the fluorescence microscope. ActD was purchased from Sigma (St. Louis, MO) and was dissolved in H_2O as a 1 mg/ml stock solution and stored at –20°C. It was added to cultures at a final concentration of 5 μg/ml. CHX (Boehringer Mannheim, Indianapolis, IN) was dissolved directly in culture medium at a concentration of 200 μg/ml and was added to cultures at a final concentration of 10 μg/ml. LMB was purchased from LC Laboratories (Woburn, MA) as a 5.4 μg/ml stock solution in ethanol and was stored at –20°C. It was diluted in culture medium and then added to cultures at a final concentration of 5.4 ng/ml (10 nM).

Fluorescence microscopy and statistical analysis of the data

Transfected cells were examined by fluorescence microscopy as described in Davidson *et al*. (2006), using a Meridian Instruments (Okemos, MI) Insight confocal laser-scanning microscope. Approximately 100 cells were scored for GFP localization: (a) N, fluorescence exclusively in the nucleus; (b) N > C, fluorescence intensely nuclear over a cytoplasmic background; (c) N ~ C, fluorescence in both the nucleus and cytoplasm; (d) N < C, less nuclear labeling than the cytoplasm; and (e) C, fluorescence exclusively in the cytoplasm. Representative cells were photographed at low magnification to show a field containing multiple cells and at high magnification to show a single cell.

The number of cells scored into each category of localization was tabulated from triplicate experiments and plotted as histograms with standard error of the mean to illustrate the fluorescence distribution. Chi-square analyses were carried out using the statistical analysis program StatView, version 5.0.1 (SAS Institute, Cary, NC). The analyses were performed using the "Contingency Table" function, selecting "Coded summary data" and deselecting "Fisher's Exact Test."

SDS–PAGE and immunoblotting

Proteins were resolved on SDS–PAGE (10% acrylamide) as described by Laemmli (1970). The procedures for immunoblotting after SDS–PAGE have also been described (Tsay *et al*., 1999). Polyclonal anti-GFP antibodies were obtained from Clontech (San Jose, CA); anti-MBP antibodies were

from New England Biolabs (Beverly, MA); and polyclonal rabbit anti-Gal3 (#32 and #33) has been described previously (Agrwal *et al*., 1993).

NES predictor server and three-dimensional visualization of Gal3

The amino acid sequence of murine Gal3, in the FASTA format (NCBI Protein Database, NCB Accession #NP_034835), was submitted to the online NES predictor server (NetNES) at the Center for Biological Sequence Analysis at the Technical University of Denmark (http://www.cbs.dtu.dk/services/NetNES/) (la Cour *et al*., 2004). Graphical and text output for the predicted NES were compared with the experimentally determined NES. Images of the CRD of Gal3 bound to *N*-acetyl lactosamine (Research Collaboratory for Structural Bioinformatics Protein Databank, PDB # 1KJL) were generated using Protein Explorer at http://proteinexplorer.org (Martz, 2002).

Acknowledgments

We thank Dr Beric Henderson, Westmead Institute for Cancer Research, New South Wales, Australia, for generous gifts of the pRev(1.4)–GFP vector and the same vector bearing the nuclear export sequences of PKI and IκBα. E.J.A. thanks Lori Keen and Stephen Matheson for their assistance with the cell culture facilities at Calvin College and Elisa Verde for Protein Data Bank searches. This work was supported by a 2003 Merck/AAAS Undergraduate Science Research Program Grant (to E.J.A.), a Calvin Research Fellowship from Calvin College (to E.J.A.), and by grants Cottrell College Science Award from the Research Corporation (to E.J.A.), GM-38740 from the National Institutes of Health (to J.L.W.), and MCB-0092919 from the National Science Foundation (to R.J.P.).

Conflict of interest statement

None declared.

Abbreviations

ActD, actinomycin D; CHX, cycloheximide; CRD, carbohydrate-recognition domain; Gal3, galectin-3; GFP, green fluorescent protein; LMB, leptomycin B; MBP, maltose-binding protein; NES, nuclear export signal; PCR, polymerase chain reaction; PDB, Protein Data Bank; PKI, protein kinase inhibitor.

References

Agrwal, N., Sun, Q., Wang, S.Y., and Wang, J.L. (1993) Carbohydrate-binding protein 35. I. Properties of the recombinant polypeptide and the individuality of the domains. *J. Biol. Chem.*, **268**, 14932–14939.

Bohnsack, M.T., Regener, K., Schwappach, B., Saffrich, R., Paraskeva, E., Hartmann, E., and Gorlich, D. (2002) Exp5 exports eEF1A via tRNA from nuclei and synergizes with other transport pathways to confine translation to the cytoplasm. *EMBO J.*, **21**, 6205–6215.

Brunet, A., Kanai, F., Stehn, J., Xu, J., Sarbassova, D., Frangioni, J.V., Dalal, S.N., DeCaprio, J.A., Greenberg, M.E., and Yaffe, M.B. (2002) 14-3-3 transits to the nucleus and participates in dynamic nucleocytoplasmic transport. *J. Cell Biol.*, **156**, 817–828.

Dagher, S.F., Wang, J.L., and Patterson, R.J. (1995) Identification of galectin-3 as a factor in pre-mRNA splicing. *Proc. Natl. Acad. Sci. U. S. A.*, **92**, 1213–1217.

Davidson, P.J., Davis, M.J., Patterson, R.J., Ripoche, M.A., Poirier, F., and Wang, J.L. (2002) Shuttling of galectin-3 between the nucleus and cytoplasm. *Glycobiology*, **12**, 329–337.

Davidson, P.J., Li, S.Y., Lohse, A.G., Vandergaast, R.V., Verde, E., Pearson, A.J., Patterson, R.J., Wang, J.L., and Arnoys, E.J. (2006) Transport of galectin-3 between the nucleus and cytoplasm. I. Conditions and signals for nuclear import. *Glycobiology*, **16**.

Fan, X.C. and Steitz, J.A. (1998) HNS, a nuclear–cytoplasmic shuttling sequence in HuR. *Proc. Natl. Acad. Sci. U. S. A.*, **95**, 15293–15298.

Gaudin, J.C., Mehul, B., and Hughes, R.C. (2000) Nuclear localisation of wild type and mutant galectin-3 in transfected cells. *Biol. Cell*, **92**, 49–58.

Hamilton, M.H., Tcherepanova, I., Huibregtse, J.M., and McDonnell, D.P. (2001) Nuclear import/export of hRPF1/Nedd4 regulates the ubiquitin-dependent degradation of its nuclear substrates. *J. Biol. Chem.*, **276**, 26324–26331.

Hauer, J.A., Barthe, P., Taylor, S.S., Parello, J., and Padilla, A. (1999) Two well-defined motifs in the cAMP-dependent protein kinase inhibitor (PKIalpha) correlate with inhibitory and nuclear export function. *Protein Sci.*, **8**, 545–553.

Heger, P., Lohmaier, J., Schneider, G., Schweimer, K., and Stauber, R.H. (2001) Qualitative highly divergent nuclear export signals can regulate export by the competition for transport cofactors in vivo. *Traffic*, **2**, 544–555.

Henderson, B.R. and Eleftheriou, A. (2000) A comparison of the activity, sequence specificity, and CRM1-dependence of different nuclear export signals. *Exp. Cell Res.*, **256**, 213–224.

Hubert, M., Wang, S.Y., Wang, J.L., Seve, A.P., and Hubert, J. (1995) Intranuclear distribution of galectin-3 in mouse 3T3 fibroblasts: comparative analyses by immunofluorescence and immunoelectron microscopy. *Exp. Cell Res.*, **220**, 397–406.

Itoh, K., Brott, B.K., Bae, G.U., Ratcliffe, M.J., and Sokol, S.Y. (2005) Nuclear localization is required for Dishevelled function in Wnt/beta-catenin signaling. *J. Biol.*, **4**, 3.

Kalland, K.H., Szilvay, A.M., Brokstad, K.A., Saetrevik, W., and Haukenes, G. (1994) The human immunodeficiency virus type 1 Rev protein shuttles between the cytoplasm and nuclear compartments. *Mol. Cell. Biol.*, **14**, 7436–7444.

Koike, M., Kose, S., Furuta, M., Taniguchi, N., Yokoya, F., Yoneda, Y., and Imamoto, N. (2004) beta-Catenin shows an overlapping sequence requirement but distinct molecular interactions for its bidirectional passage through nuclear pores. *J. Biol. Chem.*, **279**, 34038–34047.

Kudo, N., Wolff, B., Sekimoto, T., Schreiner, E.P., Yoneda, Y., Yanagida, M., Horinouchi, S., and Yoshida, M. (1998) Leptomycin B inhibition of signal-mediated nuclear export by direct binding to CRM1. *Exp. Cell Res.*, **242**, 540–547.

la Cour, T., Kiemer, L., Molgaard, A., Gupta, R., Skriver, K., and Brunak, S. (2004) Analysis and prediction of leucine-rich nuclear export signals. *Protein Eng. Des. Sel.*, **17**, 527–536.

Laemmli, U.K. (1970) Cleavage of structural proteins during the assembly of the head of bacteriophage T4. *Nature*, **227**, 680–685.

Laing, J.G. and Wang, J.L. (1988) Identification of carbohydrate binding protein 35 in heterogeneous nuclear ribonucleoprotein complex. *Biochemistry*, **27**, 5329–5334.

Lee, S.H. and Hannink, M. (2001) The N-terminal nuclear export sequence of IkappaBalpha is required for RanGTP-dependent binding to CRM1. *J. Biol. Chem.*, **276**, 23599–23606.

Lotz, M.M., Andrews, C.W., Jr, Korzelius, C.A., Lee, E.C., Steele, G.D., Jr, Clarke, A., and Mercurio, A.M. (1993) Decreased expression of Mac-2 (carbohydrate binding protein 35) and loss of its nuclear localization are associated with the neoplastic progression of colon carcinoma. *Proc. Natl. Acad. Sci. U. S. A.*, **90**, 3466–3470.

Martz, E. (2002) Protein Explorer: easy yet powerful macromolecular visualization. *Trends Biochem. Sci.*, **27**, 107–109.

McBride, K.M., McDonald, C., and Reich, N.C. (2000) Nuclear export signal located within the DNA-binding domain of the STAT1 transcription factor. *EMBO J.*, **19**, 6196–6206.

Meyer, B.E. and Malim, M.H. (1994) The HIV-1 Rev trans-activator shuttles between the nucleus and the cytoplasm. *Genes Dev.*, **8**, 1538–1547.

Michael, W.M., Choi, M., and Dreyfuss, G. (1995) A nuclear export signal in hnRNP A1: a signal-mediated, temperature-dependent nuclear protein export pathway. *Cell*, **83**, 415–422.

Michael, W.M., Eder, P.S., and Dreyfuss, G. (1997) The K nuclear shuttling domain: a novel signal for nuclear import and nuclear export in the hnRNP K protein. *EMBO J.*, **16**, 3587–3598.

Moutsatsos, I.K., Wade, M., Schindler, M., and Wang, J.L. (1987) Endogenous lectins from cultured cells: nuclear localization of carbohydrate-binding protein 35 in proliferating 3T3 fibroblasts. *Proc. Natl. Acad. Sci. U. S. A.*, **84**, 6452–6456.

Openo, K.P., Kadrofske, M.M., Patterson, R.J., and Wang, J.L. (2000) Galectin-3 expression and subcellular localization in senescent human fibroblasts. *Exp. Cell Res.*, **255**, 278–290.

Ossareh-Nazari, B., Bachelerie, F., and Dargemont, C. (1997) Evidence for a role of CRM1 in signal-mediated nuclear protein export. *Science*, **278**, 141–144.

Paces-Fessy, M., Boucher, D., Petit, E., Paute-Briand, S., and Blanchet-Tournier, M.F. (2004) The negative regulator of Gli, Suppressor of fused (Sufu), interacts with SAP18, Galectin3 and other nuclear proteins. *Biochem. J.*, **378**, 353–362.

Parra-Palau, J.L., Scheper, G.C., Wilson, M.L., and Proud, C.G. (2003) Features in the N and C termini of the MAPK-interacting kinase Mnk1 mediate its nucleocytoplasmic shuttling. *J. Biol. Chem.*, **278**, 44197–44204.

Sato, S., Burdett, I., and Hughes, R.C. (1993) Secretion of the baby hamster kidney 30-kDa galactose-binding lectin from polarized and nonpolarized cells: a pathway independent of the endoplasmic reticulum–Golgi complex. *Exp. Cell Res.*, **207**, 8–18.

Shimura, T., Takenaka, Y., Tsutsumi, S., Hogan, V., Kikuchi, A., and Raz, A. (2004) Galectin-3, a novel binding partner of beta-catenin. *Cancer Res.*, **64**, 6363–6367.

Sorme, P., Arnoux, P., Kahl-Knutsson, B., Leffler, H., Rini, J.M., and Nilsson, U.J. (2005) Structural and thermodynamic studies on cation–Pi interactions in lectin–ligand complexes: high-affinity galectin-3 inhibitors through fine-tuning of an arginine–arene interaction. *J. Am. Chem. Soc.*, **127**, 1737–1743.

Stommel, J.M., Marchenko, N.D., Jimenez, G.S., Moll, U.M., Hope, T.J., and Wahl, G.M. (1999) A leucine-rich nuclear export signal in the p53 tetramerization domain: regulation of subcellular localization and p53 activity by NES masking. *EMBO J.*, **18**, 1660–1672.

Takenaka, Y., Fukumori, T., Yoshii, T., Oka, N., Inohara, H., Kim, H.R., Bresalier, R.S., and Raz, A. (2004) Nuclear export of phosphorylated galectin-3 regulates its antiapoptotic activity in response to chemotherapeutic drugs. *Mol. Cell. Biol.*, **24**, 4395–4406.

Tsay, Y.G., Lin, N.Y., Voss, P.G., Patterson, R.J., and Wang, J.L. (1999) Export of galectin-3 from nuclei of digitonin-permeabilized mouse 3T3 fibroblasts. *Exp. Cell Res.*, **252**, 250–261.

van den Brule, F.A., Waltregny, D., Liu, F.T., and Castronovo, V. (2000) Alteration of the cytoplasmic/nuclear expression pattern of galectin-3 correlates with prostate carcinoma progression. *Int. J. Cancer*, **89**, 361–367.

Vyakarnam, A., Dagher, S.F., Wang, J.L., and Patterson, R.J. (1997) Evidence for a role for galectin-1 in pre-mRNA splicing. *Mol. Cell. Biol.*, **17**, 4730–4737.

Wen, W., Meinkoth, J.L., Tsien, R.Y., and Taylor, S.S. (1995) Identification of a signal for rapid export of proteins from the nucleus. *Cell*, **82**, 463–473.

Xiao, Z., Watson, N., Rodriguez, C., and Lodish, H.F. (2001) Nucleocytoplasmic shuttling of Smad1 conferred by its nuclear localization and nuclear export signals. *J. Biol. Chem.*, **276**, 39404–39410.